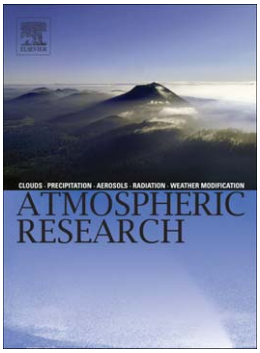

Quantifying the relationship between extreme air pollution events and extreme weather events

Henian Zhang, Yuhang Wang, Tae-Won Park, Yi Deng

PII: S0169-8095(16)30609-3
DOI: doi: 10.1016/j.atmosres.2016.11.010
Reference: ATMOS 3837

To appear in: *Atmospheric Research*

Received date: 25 June 2016
Revised date: 14 November 2016
Accepted date: 15 November 2016

Please cite this article as: Zhang, Henian, Wang, Yuhang, Park, Tae-Won, Deng, Yi, Quantifying the relationship between extreme air pollution events and extreme weather events, *Atmospheric Research* (2016), doi: 10.1016/j.atmosres.2016.11.010

Quantifying the Relationship between Extreme Air Pollution Events and Extreme Weather Events

Henian Zhang[1,*], Yuhang Wang[1], Tae-Won Park[1,2], and Yi Deng[1]

[1]Georgia Institute of Technology, Atlanta, GA, USA

[2]Chonnam National University, Gwangju, South Korea

*Corresponding author. Email address: henian.zhang@eas.gatech.edu (H. Zhang).

Abstract

Extreme weather events can strongly affect surface air quality, which has become a major environmental factor to affect human health. Here, we examined the relationship between extreme ozone and PM2.5 (particular matter with an aerodynamic diameter less than 2.5 μm) events and the representative meteorological parameters such as daily maximum temperature (Tmax), minimum relative humidity (RHmin), and minimum wind speed (Vmin), using the location-specific 95th or 5th percentile threshold derived from historical reanalysis data (30 years for ozone and 10 years for PM2.5). We found that ozone and PM2.5 extremes were decreasing over the years, reflecting EPA's tightened standards and effort on reducing the corresponding precursor's emissions. Annual ozone and PM2.5 extreme days were highly correlated with Tmax and RHmin, especially in the eastern U.S. They were positively (negatively) correlated with Vmin in urban (rural and suburban) stations. The overlapping ratios of ozone extreme days with Tmax were fairly constant, about 32%, and tended to be high in fall and low in winter. Ozone extreme days were most sensitive to Tmax, then RHmin, and least sensitive to Vmin. The majority of ozone extremes occurred when Tmax was between 300 K and 320 K, RHmin was less than 40%, and Vmin was less than 3 m/s. The number of annual extreme PM2.5 days was highly positively correlated with the extreme RHmin/Tmax days, with correlation coefficient between PM2.5/RHmin highest in urban and suburban regions and the correlation coefficient between PM2.5/Tmax highest in rural area. Tmax has more impact on PM2.5 extreme over the eastern U.S. Extreme PM2.5 days were more likely to occur at low RH conditions in the central and southeastern U.S., especially during spring time, and at high RH conditions in the northern U.S. and the Great Plains. Most extreme PM2.5 events occurred when Tmax was between 300 K

and 320 K and RHmin was between 10% and 50%. Extreme PM2.5 days usually occurred when Vmin was under 2 m/s. However, during spring season in the Southeast and fall season in Northwest, high winds were found to accompany extreme PM2.5 days, likely reflecting the impact of fire emissions.

1. Introduction

In recent decades, air pollution has become a major environmental risk to human health [World Health Organization (WHO), 2014]. Globally, outdoor air pollution was estimated to cause 3.7 million premature deaths per year. Ozone and PM2.5 (particular matter with an aerodynamic diameter less than 2.5 μm) are two of the most widespread air pollutants. Ground level ozone may cause irritation of the respiratory system, decrements in lung function, inflammation and damage to the airways [Environmental Protection Agency (EPA), 2007]. A 0.52% overall excess risk in non-accidental daily mortality was reported by Bell et al. (2004) for each 10-ppb increase in the previous week's ozone for 95 large U.S. communities over the period of 1987 to 2000. Exposure to high concentration of PM2.5 for prolonged periods can lead to serious health effects such as decreased lung function, chronic bronchitis, and premature death (Pope and Dockery, 2006; EPA, 2005). Short-term exposures may increase the risk for respiratory symptoms, cardiac arrhythmias, and heart attacks. Children, older adults, and people with heart and lung diseases are at greater risk. According to Caiazzo et al. (2013), changes in PM2.5 and ozone concentrations account for about 200,000 and 10,000 premature deaths each year in the U.S., respectively.

Meteorological processes on various spatial and temporal scales strongly affect air quality including ozone and PM2.5 concentrations. Through various weather processes, major meteorological parameters that can affect ozone include ultraviolet (UV) radiation, cloud cover, temperature, wind direction and speed, precipitation, and position of fronts (Tang et al., 2009). Meteorological factors that may affect PM2.5 include wind field, position of high pressure system, relative humidity (RH), mixing height, atmospheric stability, and temperature (Dawson et al., 2014). Extreme weather events such as heat waves, droughts, and air stagnation are

particularly important when air pollutants can accumulate over a relatively long time period during the event. Through various weather processes, climate change may directly affect air quality by modulating emission inventories and dispersion patterns. Changes in duration, frequency, and spatial extent of weather extremes have been reported by the Intergovernmental Panel on Climate Change (IPCC, 2007). For example, heat waves may become more frequent over most land areas causing high temperature, more biogenic emission, and faster chemical reaction that contribute to high ozone and PM2.5 concentrations. Extra-tropical storm tracks may move poleward and cause temperature/wind/precipitation pattern shifts. Understanding the impact of extreme weather on air quality in a changing climate becomes crucial. Tagaris et al. (2009) estimated that ozone and PM2.5 related health issues such as premature mortality, respiratory diseases, and cardiovascular diseases may increase in the most densely populated areas in the future, although large uncertainties in climate models, emission inventories, and the assumptions used for population distributions were acknowledged. In order to improve future climate projection, understanding the relationship between the air pollution events and extreme weather events in the past became an important step.

To address this need, we presented here a quantitative study of the extreme air pollution events and extreme weather events based on historical observations. In particular, we examined the relationship between extreme ozone/PM2.5 events and the representative meteorological parameters such as temperature, RH, and wind speed. Occurrences of extreme weather events and extreme ozone/PM2.5 events were analyzed in a synchronized manner. The duration, frequency, magnitude, and spatial-temporal scales of extreme events were examined.

2. Methodology

Thompson et al. (2001) provided a comprehensive review of a variety of statistical methods for meteorological adjustment of ozone, which can be classified into regression, extreme value, and space-time methods. The most commonly used method is the parametric linear regression (Eder et al., 1994; Bloomer et al., 2009; Tai et al., 2010). However, the resulted linear correlation varies by location and time period. Therefore, more sophisticated methods such as nonlinear regression (Bloomfield, 1996; Niu, 1996), time-series modeling (Rao et al., 1997), and spatial-temporal modeling (Carroll et al., 1997) were proposed. Thompson et al. (2001) concluded that "no method is most appropriate for all purposes and all scenarios."

Here, we examined a new approach to quantify the relationship between air quality extremes and weather extremes. IPCC Data Distribution Center (DDC) defines an extreme weather event as "An event that is rare at a particular place and time of year. Definitions of rare vary, but an extreme weather event would normally be as rare as or rarer than the 10th or 90th percentile of a probability density function estimated from observations." Here, we defined "extreme event" as an event having less than the lowest or highest 5% of occurrences for the selected analysis period. For air quality parameters, the 8-hr maximum ozone concentrations and PM2.5 24-hr geometric mean derived from the EPA Air Quality System (AQS) were used. All four AQS designated stations types (rural, urban, suburban, and unknown) were included. The ozone data covered a 30-yr period from 1980 to 2009 and the PM2.5 data covered a 10-yr period from 2000 to 2009. Only AQS stations that have data coverage of more than 20% of the selected period were used. Meteorological parameters including daily maximum temperature (Tmax), daily minimum RH (RHmin), and daily minimum wind speed (Vmin) from the National Centers for Environmental Protection (NCEP) Climate Forecast System Reanalysis (CFSR) time series

(0.3^{o}x0.3^{o}) were used in this analysis to quantify weather extremes. Meteorological data from the grid point closest to a given AQS station were chosen for pairing with the air quality events directly. Table 1 listed the air quality indices and meteorological parameters selected for this study.

The typical time scale of a low frequency weather regime is usually 10 to 30 days with an average of 20 days. Here, we used a 21-day window centered on the selected date for a particular station that extended to all available historical data, and defined the top 95th or bottom 5th percentile (depending on the parameters) as the threshold for defining air quality or weather extreme. In particular, we used the 95th percentile of daily Tmax, 5th percentile of daily RHmin, and 5th percentile of daily Vmin to define the extreme Tmax/RHmin/Vmin days, and 95th percentile of ozone and PM2.5 concentrations to define the extreme ozone/PM2.5 days. High temperature, low RH, and low wind speed represent a hot, dry, and stagnant weather condition. This condition is favorable for ozone and PM2.5 formation and accumulation under most circumstances, which has been demonstrated later on in our analysis. For example, to determine whether or not a given day is considered an extreme ozone day, the following steps were taken: extract the ozone data from a station for that day and plus/minus 10 days (21 days in total) for the entire analysis period (30 years for ozone); sort the array and determine the 95th percentile; and if the concentration of that day is greater than the 95th percentile, that day is considered an extreme ozone/PM2.5 day for that station.

We further divide the AQS stations into four zones: the Northwest, the Northeast, the Southeast, and California to investigate the regional variability. In addition, the 30-year ozone data were divided into three decades in selected analysis to examine the decadal variability. The 21 days window was only applied to the specific 10 years in each decade to derive the extreme

threshold. Therefore, for a given station, the 95th percentile threshold of the 80s will be different from that of the 90s.

To evaluate the effect of a weather extreme event that lasts three or more days, we further defined heat wave event, dry event, and low wind event. A heat wave event was defined as any event having three or more consecutive days with Tmax equal to or greater than the extreme Tmax index. Any day part of a heat wave event is defined as a heat wave day. Similarly, a dry event (low wind) event was an event with RHmin (Vmin) equal to or less than the extreme RHmin (Vmin) index. The dry event day and low wind event day were defined in a similar manner. The overlapping days between extreme Ozone/PM2.5 days and heat wave/dry event/low wind event day will be explored.

The advantage of using 5th or 95th percentile values derived from multi-year data as the extreme event threshold is that the threshold varies from station to station and from time to time. It depends on historical values rather than a fixed pre-determined index. It is more site-relevant compared to some traditional ways to define weather extreme and air pollution index. For example, the National Weather Service (NWS) excessive heat watch and warning system requires daytime heat index greater than or equal to 40.6^{o}C (105^{o}F), with nighttime lows greater than or equal to 26.7^{o}C (80^{o}F), for two consecutive days. The daytime heat index is a function of temperature and RH (Robinson 2001). Used by the National Oceanic and Atmospheric Administration (NOAA) National Centers for Environmental Information (NCEI), Air Stagnation Index refers to the percentage of days with air stagnation conditions which are described as sea level geostrophic wind speed less than 8 m/s for at least 4 days with no precipitation or the wind speed at 500 mb exceeding 13 m/s (Wang and Angell, 1999). These indices can provide a quick snap shot of the spatial and temporal trend of extreme weather

events. However, using the same threshold values for all sites lead to regional biases of extreme event occurrence. The difference of regional biases among air quality and weather extremes makes it impractical to analyze their relationships. For example, the NOAA excessive heat watch warning occurs more frequently in southern than northern U.S. due to regional temperature difference. Summertime ozone concentrations tend to be higher in California (CA) and Northeast than other regions. Our method of using locally defined 95th or 5th percentile value as a threshold provides a consistent analysis across the regions. However, one drawback of this approach is that it relies heavily on data temporal and spatial coverage and involves large amounts of historical data analysis, which can be computationally expensive for near real-time analyses.

3. Results

3.1. Quantifying the relationship between the extreme ozone events and extreme weather events

Surface ozone concentrations may be affected by many factors such as UV radiation, cloud cover, temperature, wind direction and speed, precipitation, and position of fronts. In general, ozone tends to be high when air is warm, dry, and stagnant. However, there are exceptions. For example, horizontal advection may spread ozone to stations downwind. Vertical mixing may help bring ozone from upper level down to the surface. Cold and stagnant air in winter, especially with snow cover on the ground, creates favorable conditions for ozone formation. Snow cover further reduces the deposition rate of ozone to the ground. Many local factors can also contribute to ozone extremes. Figure 1a shows the annual variability of extreme ozone days from 1297 AQS stations that have data coverage of more than 20% of the entire 30-year period. Meteorological data from grid points closest to the 1297 AQS stations for the 30-year period

were used to derive the weather extreme indices. The extreme ozone days decreased significantly since 2003 despite of the increase of AQS stations during this period. This is consistent with previous analysis such as Cooper et al. (2012) and EPA Regulatory Impact Analysis (2014). According to several recent studies (Frost et al., 2006; Kim et al., 2006; Gilliland et al., 2008; Butler et al., 2011), the reduction in precursor trace gases such as NOx, CO, and volatile organic carbons (VOCs) regulated by EPA were responsible for the downward trend. In the past two decades, to protect public health, EPA has tightened the 8-hour "primary" ozone standard from 0.084 ppm in 1997 to a level of 0.075 ppm in 2008. In 2015, a new National Ambient Air Quality Standards (NAAQS) for ozone was proposed, which further reduced the ozone standard to 0.070 ppm. With the new rule implemented, a further reduction of ground level ozone may be achieved.

Figure 1b shows the number of extreme Tmax days changing over the years. Jacob and Winner (2009) pointed out that of all meteorological variables, temperature affects ozone trends the most in polluted regions due to air mass stagnation and strong sunlight associated with high temperature. Therefore, surface ozone concentration was highly correlated with high temperature in the eastern U.S. (Bloomer et al., 2009). Here, we observe a strong correlation between annual extreme Tmax and ozone days with the correlation coefficient of 0.532 at the 99% significance level (Table 2a). High correlations mostly occurred in the Northeast and Southeast (Fig. 2a). A slightly higher correlation of 0.548 at 99% significance level was found between the extreme ozone days (Fig. 1a) with heat wave days (Fig. 1e). The positive correlation implies when the number of extreme Tmax days in a year increases, the ozone extremes will likely increase. According to IPCC (2007) and Melillo et al. (2014), heat wave days are increasing in recent

years. If the increasing trend continues, more ozone extremes and more ozone related premature deaths are likely to occur, which is consistent with the findings of Tagaris et al. (2009).

Annual total ozone extreme days were also strongly associated with RHmin extremes (Fig. 1c). The correlation coefficient was 0.54 with extreme RHmin days and 0.53 with dry event days, both at the 99% significance level. Model simulations showed that ozone production often reaches maximum under the warmest and driest condition (Goliff et al., 2013). Lower RH indicates a lower chance for cloud and precipitation formation, although the overall impact of cloud on ground ozone concentrations can be difficult to assess (Barth et al., 2007). Similar to Tmax, high correlation of RHmin and ozone extreme days mainly occurred in the Northeast and Southeast (Fig. 2b). Overall, both extreme Tmax and RHmin days had a significant impact on extreme ozone days on an annual basis.

The total extreme Vmin days showed a slight increasing trend over the past 30 years (Fig. 1d). This is consistent with the finding that the number of summer stagnant days is on the rise (Horton et al., 2012). The correlation coefficient between the extreme Vmin days and ozone extremes was −0.282 with a significance level of 80%, which indicates more low wind days in a year may correlate to less ozone extremes. At first, this may be counter-intuitive. However, when looking at the spatial distribution of the correlation in detail (Fig. 2c), we found that majority of the negative correlation occurred in rural and suburban areas where high ozone concentration was not due to local production but transport. Low wind may slow down the transport of ozone from high emission areas. Low wind also indicates stagnant air mass and less vertical mixing, which may reduce the efficiency of deposition of ozone near the surface and the chance of ozone from the upper levels being entrained downward (Klingberg et al., 2012; Zhang and Rao, 1999). The correlation coefficient was −0.495 averaged over the rural stations (a total of 489 stations)

and −0.316 averaged over the suburban stations (a total of 534 stations). On the other hand, large cities, where ozone concentrations are affected more by local sources, low wind typically leads to high ozone concentration with a correlation coefficient of 0.201 averaged over the 248 urban stations. Since there are more rural and suburban stations, the overall averaged correlation coefficient is negative. The increasing trend of Vmin days and a decreasing trend of ozone extreme observed during the past 30 years also contributed to the overall negative correlation coefficient.

We further separated the extreme ozone and weather event days into three decades (80s, 90s, and 00s) and four seasons (winter: December-January-Feburary (DJF); spring: March-April-May (MAM); summer: June-July-August (JJA); and fall: September-October-November (SON)) (Figure 3). For the decadal variability analysis, the 21−day window was only applied to the specific 10 years to derive the extreme threshold. There were more stations available in the 00s than in the 80s, and 90s (Table 1). Therefore, more ozone extremes were recorded (Fig. 3a). Similarly, for seasonal variations, only days from a particular season were chosen. Since there were more stations operating in summer (Table 1), more ozone extremes were recorded in JJA than any other season (Fig. 3a). Figure 3b shows the numbers of extreme Tmax/RHmin/Vmin days for the three decades and four seasons. The numbers of extreme days are the same for the three variables since they were either top or bottom 5% of the NCEP CFSR data. Overall, overlapping ratio was found to be the highest with Tmax extreme days (Fig. 3f), and lowest with Vmin extreme days (Fig. 3h), which means ozone extreme is most sensitive to Tmax and least sensitive to Vmin. The overlapping ratios with the top 5% Tmax extreme remained constant about 32% for the entire 30-year period, 80s, 90s, and 00s. The overlapping ratio with the medium and lowest 5% Tmax days dropped significantly to less than 2% and less than 0.5%,

respectively. The overlapping ratio exhibited strong seasonal variability with the highest value found in spring and fall (Fig. 3f) despite the fact that the number of extreme ozone events was the highest in summer (Fig. 3a). Figure 4 shows the spatial distributions of the overlapping ratios for the entire 30-year period and four seasons. Overlapping ratio for ozone extreme with extreme Tmax days was found to be highest in California, Northwest and Northeast U.S. during spring (Fig. 4g) and fall (Fig. 4m).

The overlapping ratio of the ozone extreme days also increased with decreasing RHmin (Fig. 3g). The overlapping ratio of ozone extreme to the extreme RHmin days increased slightly from 19% in the 80s to 22% in the 00s (Fig. 3g). The overlapping ratio was the highest in fall and lowest in winter. High correlation of the ozone extreme and RHmin extreme can be seen nationwide (Fig. 4b) especially for the Northwest and Eastern U.S. during spring, summer, and fall.

Ratio of overlapped events with Vmin remained low for most part of the U.S. and for all four seasons (Fig. 4c, 4f, 4j, 4l, and 4o). Fig. 3e and 3h showed that about 9% of ozone extreme days co-occurred with the lowest 5% Vmin days, 5% co-occurred with the medium 5% Vmin days, and less than 1% co-occurred with the highest 5% Vmin days. Compared to the reduction of ozone extreme with decreasing Tmax, the reduction of ozone extremes with increasing Vmin is less significant. A few stations in the western states (Idaho, Nevada, Utah, and Colorado) even have a high ratio of ozone extreme overlapping with high wind days in winter time (figure not shown). One explanation is that increasing wind speed may increase the efficiency of ozone surface deposition, promote vertical mixing, and bring ozone from upper levels (such as the nocturnal residual layer) down to the surface (Klingberg et al., 2012; Zhang and Rao, 1999). In extreme case, stratospheric intrusion may occur, which is usually associated with intense surface

and upper-level low pressure systems causing stratospheric ozone mixing with surface air (Oltmans and Levy, 1992; Appenzeller and Davies, 1992). If an ozone exceedance occurred during the stratospheric intrusion, it must be documented by states as an exceptional event not counted as nonattainment.

Figure 5 shows the variation of ozone extreme days averaged for different time periods. It can be seen that over the 30-year period (Fig. 5a), southern California experienced the biggest reduction for ozone extreme, while Florida and Texas experienced a slight increase. If breaking down to three decades, the increasing trend for most part of U.S. mostly occurred during the first two decades (Fig. 5b and 5c). From 2000 to 2009, a reduction of ozone extreme days was observed nationwide (Fig. 5d). For California, an increasing trend can be observed from 1980 to 1989. For the period of 1990 to 1999, although rest of the country was experiencing a dramatic increase reflecting the economic boom, the majority of stations in California showed a reduction of extreme ozone events due to its effort as the leading state in regulating ozone emission.

To examine the relative importance of each meteorological parameter to ozone extreme, Figure 6 shows the joint Probability Density Function (PDF) of ozone extreme event as functions of Tmax and RHmin, Tmax and Vmin, and RHmin and Vmin averaged for the entire 30 years and four seasons. Figure 7 shows the regional and seasonal variability of the joint PDF for ozone extreme days with respect to the most sensitive parameters, Tmax and RHmin. The PDF of ozone extreme with respect to various meteorological parameters varied little from decade to decade, therefore related figures were not shown. The bin size is 5 K for Tmax, 3.33% for RHmin, and 1 m/s for Vmin. The value represents the percentage fractions of extreme ozone days out of the total number of days with ozone observations within each bin. To be statistically significant, only bins having more than 100 days of ozone observations were included. Averaged

over the entire 30-year period, the majority of ozone extreme days occurred when Tmax was between 300K and 320K, RHmin was less than 40% and Vmin less than 3 m/s. In winter, a second peak can be found in all four regions when Tmax was around 265 K, Vmin was near 10 m/s, and RHmin was above 90%. This condition may indicate snow on the surface together with horizontal advection and perhaps, vertical mixing. Snow covered ground may reduce the deposition rate of surface ozone (Galbally and Roy 1980; Garland and Derwent 1979). Its high albedo also helps enhance the UV radiation (Schnell et al., 2009). Strong wind may help bring pollutant from other regions or upper levels down to the surface. Overall, Ozone extreme days were most sensitive to Tmax, followed by RHmin, and least sensitive to Vmin.

3.2. Quantifying the relationship between the extreme PM2.5 events and extreme weather events

PM2.5 in the atmosphere is produced by various sources such as fire, industrial and residential combustion, agriculture, stone crushing, unpaved roads, and vehicle exhaust (EPA, 2004). The major species are carbon, sulfate and nitrate compounds, soil, and ash (Liu et al., 2005; Bell et al., 2007). The composition varies greatly from region to region and from season to season (Bell et al., 2007). In addition to primary emissions, secondary PM2.5 may form due to chemical oxidation in the atmosphere.

The relationship between PM2.5 and meteorological conditions can be complex. High temperature may increase production of sulfate from SO_2 through secondary aerosol formation (Sheehan and Bowman, 2001), but decrease the amount of semi-volatile particulate as their saturation vapor pressure increases (Aw and Kleeman, 2003). Higher RH promotes the formation of sulfate and nitrate, but overall, precipitation causes a reduction of PM2.5 through scavenging (Koch et al., 2003). Weather system that lasts a prolonged period of time can have a profound

impact on regional PM2.5 concentrations. Low pressure system may bring heavy precipitation and strong winds. Scavenging and rapid ventilation of pollutants by these systems reduce PM2.5 concentrations significantly. In some cases, particle (such as wind-blown dust) concentration may increase briefly when weather front passes through and then decrease (Feng and Wang, 2012). On the other hand, high pressure system brings calm and clear sky conditions that lead to excessive radiative cooling and strong near-surface inversion during nighttime. The reduced ventilation and shallow boundary layer at night tend to increase daily average PM2.5 concentrations and promote nitrate formation. Human activities in response to natural variations further complicated the picture. For example, during hot summer days, increasing demand of electricity for cooling may cause increase in sulfur dioxide emission from power plant, which is the precursor for sulfate formation. In the eastern U.S., sulfates accounts for 25% to 55% of total annual PM2.5 with power plants contributing the most (EPA, 2004).

PM2.5 24-hr geometric mean concentrations derived from the EPA AQS was used for the PM2.5 analysis. The data covered a 10-yr period from 2000 to 2009. Seen from Fig. 8a, the number of extreme PM2.5 days generally decreased during the 10 years from 2000 to 2009 with the exceptions of year 2001, 2005, and 2007. This decreasing trend reflects the effectiveness of EPA's more stringent standards for PM2.5 and emission control of the precursors over the years. In 1997, EPA set the annual standard at 15 $\mu g/m^3$ and 24-hr standard at 65 $\mu g/m^3$. EPA strengthened the 24-hr standard from 65 to 35 $\mu g/m^3$ in 2006 and the annual standard from 15 to 12 $\mu g/m^3$ in 2012. Nearly one-third of the PM2.5 reduction in the eastern U.S. can be attributed to sulfates reduction (EPA, 2004). Reduction of carbon-containing particles contributed a significant portion in PM2.5 improvement, especially in the Midwest and Southeast.

The number of annual extreme PM2.5 days was highly correlated with extreme RHmin days (Fig. 8c) with a correlation of 0.722 at 95% significance level (Table 2b), which means that when the number of low RHmin days in a year increases, the number of PM2.5 extreme events increases. The correlation was found highest in suburban and urban stations. Correlation coefficient between the extreme PM2.5 and Tmax days was 0.559 at 90% significance level with the highest correlation found in rural area. The positive correlation between PM2.5 and RHmin/Tmax can be seen nationwide over majority of the stations (Fig. 9a and 9b), especially in the eastern U.S. Extreme PM2.5 days were negatively correlated with Vmin days with a correlation coefficient of –0.504 at 80% significance level (Table 2b), which means for most stations, when the number of extreme Vmin days increases over the 10 years as seen in Fig. 8d, the number of extreme PM2.5 days decreases as seen in Fig. 8a. The highest correlation was found in rural area and lowest correlation was found in urban area (Table 2b). Similar to ozone, the relationship between PM2.5 and Vmin can be complex. If local sources are insignificant in rural area, low wind will less likely transport pollution from other nearby major sources.

The number of PM2.5 stations remained fairly constant from season to season (Table 1 and Fig. 10a). About 20% of PM2.5 extreme events occurred when Tmax was in the top 5% range (Fig. 10f), of which most occurred during the spring, summer, and fall. In winter, the medium 5% of Tmax had the highest overlapping ratio with PM2.5 extreme days. The overlapping ratios for extreme PM2.5 and RHmin days varied greatly from season to season (Fig. 10g). During summer and fall, PM2.5 extreme days tended to occur when RHmin was in the bottom 5% indicating less precipitation. However, during the winter and spring, PM2.5 extreme occurred more often when RHmin was high. The reason is that at low temperatures, high RH may significantly enhance the sulfate formation from coal-fired power plant emission (Dittenhoeffer

and De Pena, 1978; Liebsch and De Pena, 1982) and ammonium nitrate formation (Stelson and Seinfeld, 1982), especially during periods with snow cover (Green et al., 2015). About 9% of PM2.5 extreme occurred when Vmin was in the bottom 5% range (Fig. 10h).

Figure 11 shows the spatial distributions of the overlapping ratio between PM2.5 and various meteorological parameters. Besides California and a few stations in the Northwest, all stations showed that most extreme PM2.5 events occurred when Tmax was in the top 5% range (Fig. 11a). High temperature has more impact over the eastern U.S. than the western U.S. PM2.5 extreme showed high overlapping ratios in south central and southeast U.S. when RHmin was in the bottom 5% (Fig. 11f). When RHmin was in the top 5%, northern U.S. and the Great Plains had more PM2.5 extreme days (Fig. 14d). This is due to high RH may significantly enhance the sulfate formation from power plant emission and ammonium nitrate formation during winter and spring. High RH also helps promote sulfate formation through in-cloud SO_2 oxidation associated with the moist southerly flow and ammonia nitrate formation from ammonia emitted from agricultural activities in the Midwest and Great Plains during spring and summer (Aneja et al., 2003). Extreme PM2.5 events were more likely to occur when Vmin was low (Fig. 11i), especially in urban and suburban stations, and less likely to occur when Vmin was high (Fig. 11g). Most stations having more PM2.5 extreme on high wind days (Fig. 11g) had less PM2.5 extreme on low wind days (Fig. 11i), which suggests that the PM2.5 measured at these stations were not produced locally, but somewhere upwind.

The overall trend of the extreme PM2.5 days was shown in Fig. 12. Most of the 788 stations recorded a decreasing trend at high confidence level. Many of the stations in the Great Plains showing increasing trend had increased activity of oil production (Prenni et al., 2016). The PDF analysis shows that most extreme PM2.5 events occurred when Tmax was between 300 K and

320 K, RHmin was between 10% and 50%, and Vmin was under 2 m/s (Fig. 13). A second peak was found on Fig. 13a when RHmin was close to 100% and Tmax was around 270 K. If breaking down into different seasons, the second peak was found during winter (Fig. 13d), spring (Fig. 13g) and fall (Fig. 13m) in the Northwest and Northeast (figure not shown). This may be associated with sulfate and nitrate formation enhanced by high RH and low temperatures.

Extreme PM2.5 days usually occurred when Vmin was under 2 m/s (Fig. 13b), except for spring (Fig. 13h) and fall (Fig. 13n), when a second peak with Vmin at about 5 m/s and Tmax at about 305 K appeared. Regional analysis showed that spring season in the Southeast and fall season in the northwest contributed most to the second peak. This was likely associated with burning, especially prescribed burning in the Southeast (Zeng et al., 2008; Zeng and Wang, 2011) as wind may help distribute pollutants over a larger area affecting more stations.

4. Conclusions and implications for climate projection

Here, we developed a new statistical method to quantify the air quality and weather extremes using the 95th or 5th percentile threshold derived from historical data (30 years for ozone and 10 years for PM2.5). This method is more objective and provides a consistent analysis across different regions. The 95th or 5th percentile threshold varied from station to station and from time to time in order to account for seasonal and regional variability. We found that ozone extremes were decreasing over the past 30 years with a steeper slope in the last 10 years. Southern California experienced the biggest reduction of ozone extremes while Florida and Texas experienced a slight increase. Ozone extremes were highly positively correlated with the Tmax with the highest correlation found in the eastern U.S. The overlapping ratios of ozone and Tmax extreme days were fairly constant at about 32% for the 80s, 90s, 00s, and entire 30-year period. The overlapping ratios of ozone and Tmax extremes were found to be highest in fall and

lowest in winter. The highest overlapping ratios were found in California, the Northwest, and Northeast. The ozone extreme days were most sensitive to Tmax, then RHmin, and least sensitive to Vmin. Therefore, ozone extreme trend may be most likely to be determined by the temperature variation. According to the most recent national climate assessment (Melillo et al., 2014), the average U.S. temperature is projected to increase by about 3 to 12°F by the end of 2100 depending on the numerical model and emission scenario. The number of days with maximum temperature greater than 90°F is expected to increase throughout the U.S., which indicates more extreme Tmax days and more frequent and intense heat waves. This may increase the background ozone concentration and make it more difficult for EPA to reaching its goal, especially for urban stations in the northeastern U.S.

About 20% of the extreme ozone events occurred when RHmin was in the lowest 5% range. Ozone extremes in a year were also found to be highly positively correlated with the RHmin with the highest correlation found in the eastern U.S during summer and fall. According to Melillo et al. (2014), summer droughts are expected to intensify over most part of the U.S., which may increase the ozone extremes during this time.

Ozone extremes were positively correlated with Vmin in urban stations, and negatively correlated with Vmin in rural and suburban stations, which means the ozone concentrations tend to increase when more stagnant days occur at urban stations or more non-stagnant days occur at rural and suburban stations. Climate projection of stagnant days at different type of stations will help understand the future impact of Vmin on ozone extremes.

Averaged over the 30-year period, the majority of ozone extremes in the U.S. occurred when Tmax was between 300 K and 320 K, RHmin was less than 40%, and Vmin was less than 3 m/s. A secondary high can be found when RHmin was greater than 90% and Tmax was around 265 K

in winter, which may be associated with snow on the surface. According to Melillo et al. (2014), the length of time with snow cover on the ground has become shorter. The role of snow on increasing surface ozone concentration may become less significant.

PM2.5 extremes have been decreasing over the past 10 years. Most extreme PM2.5 events occurred when Tmax was between 300 K and 320 K, RHmin was between 10% and 50%, and Vmin was below 2 m/s. The number of annual extreme PM2.5 days was highly positively correlated with the extreme RHmin/Tmax days, which means that when the number of extreme RHmin/Tmax days in a year increases, the number of PM2.5 extreme events will likely increase. If global temperature increases as projected, the eastern U.S. will likely to see an increase of PM2.5 extremes, especially for the Northeast. The correlation coefficient between PM2.5 and RHmin was highest in urban and suburban regions and the correlation coefficient between PM2.5 and Tmax was highest in rural areas, which means the urban/suburban areas were most sensitive to the increase in extreme RHmin days and the rural area was most sensitive to increase in extreme Tmax days. According to Melillo et al. (2014), the northern U.S. may receive more precipitation during winter and spring, which may help remove PM2.5 from the atmosphere.

The number of PM2.5 extreme days was negatively correlated with extreme Vmin days with rural areas having the highest value, which means that low winds will less likely transport pollution to rural stations. If the number of stagnant days during summer increase as reported by Horton et al. (2012), more extreme PM2.5 days will be likely to occur in urban areas and less likely to occur in rural and suburban areas.

The PM2.5 extremes exhibited strong seasonal and regional variabilities affected by human and natural activities such as farming in the Midwest and Great Plains during spring and summer, prescribed burning in the Southeast during spring, wildfires in the Northwest during

summer and fall, biogenic emissions in the South during summer, and emission from power plants. Heat waves and summer droughts are projected to become more and more frequent (Melillo et al., 2014), which will affect and be affected by these activities. Climate projection must consider different scenarios for these activities.

Quantifying the relationship between the extreme air pollution and extreme weather events using historical data is an important step toward understanding the trend of air quality extremes in a changing climate. Although fewer ozone and PM2.5 extremes were observed in recent years as a result of EPA's effort on emission control, more studies need to be conducted to improve our understanding of the impact of climate change for different regions under different emission scenarios. The proposed method will help reveal important relationships between weather and air quality extremes on various spatial and temporal scales. It is more objective and less dependent on station location and time of year compared to previous methods of using the same criteria for the contiguous U.S. Further analysis such as using PM2.5 composition data will reveal more information on the impacts of a certain weather system on a particular pollutant although data coverage might be a challenge. Quantification of the relationship between weather and air quality extremes will help us obtain a probabilistic projection for future air quality events, reduce uncertainties from the numerical models, and provide improved understanding for stakeholders and policy makers.

Acknowledgments

This work was supported by the U.S. EPA (Grant R835204). Tae-Won Park was also supported by the National Research Foundation of the Korean government (Grant NRF-2015R1D1A1A01058100) and the Korea Meteorological Administration Research and Development Program (KMIPA2015-2091). The author would like to thank Yongjia Song for

providing the AQS ozone and PM2.5 data and Zhenzhen Yin for conducting preliminary analysis. The views presented do not necessarily represent those of the U.S. EPA.

References

Aneja, V.P., Nelson, D., Roelle, P.A., Walker, J., Battye, W., 2003. Agricultural ammonia emissions and ammonium concentration associated with aerosols and precipitations in the Southeast United States. J. Geophys. Res. 108, ACH 12-1 to 12-11.

Appenzeller, C., Davies, H. C., 1992. Structure of stratospheric intrusions into the troposphere. Nature, 358(6387), 570–572,

Aw, J., Kleeman, M.J., 2003. Evaluating the first-order effect of intraannual temperature variability on urban air pollution. J. Geophys. Res. 108, No. D12, 4365.

Barth, M.C., Kim, S.-W., Wang, C., Pickering, K.E., Ott, L.E., Stenchikov, G., Leriche, M., Cautenet, S., Pinty, J.-P., Barthe, C., Mari, C., Helsdon, J., Farley, R., Fridlind, A.M., Ackerman, A.S., Spiridonov, V., Telenta, B., 2007. Cloud-scale model intercomparison of chemical constituent transport in deep convection. Atmos. Chem. Phys. 7, 4709–4731.

Bell, M.L., McDermott, A., Zeger, S.L., Samet, J.M., Dominici, F., 2004. Ozone and short-term mortality in 95 US urban communities, 1987-2000. J. Am. Med. Assoc. 292, 2372–2378.

Bell, M.L., Dominici, F., Ebisu, K., Zeger, S.L., Samet, J.M., 2007. Spatial and temporal variation in $PM_{2.5}$ chemical composition in the United States for health effects studies. Environ. Health Perspect. 115, 989–995.

Bloomer, B.J., Stehr, J.W., Piety, C.A., Salawitch, R.J., Dickerson, R.R., 2009. Observed relationships of ozone air pollution with temperature and emissions. Geophys. Res. Lett. 36, L09803.

Bloomfield, P.J., Royle, J.A., Steinberg, L.J., Yang, Q., 1996. Accounting for meteorological effects in measuring urban ozone levels and trends. Atmos. Environ. 30, 3067–3077.

Butler, T.J., Vermeylen, F.M., Rury, M., Likens, G.E., Lee, B., Bowker, G.E., McCluney, L., 2011. Response of ozone and nitrate to stationary source NOx emission reductions in the eastern USA. Atmos. Environ. 45, 1084–1094.

Caiazzo, F., Ashok, A., Waitz, I.A., Yim, S.H.L., Barrett, S.R.H., 2013. Air pollution and early deaths in the United States. Part I: Quantifying the impact of major sectors in 2005. Atmos. Environ. 79, 198–208.

Carroll, R.J., Chen, R., George, E.I., Li, T.H., Newton, H.J., Schmiediche, H., Wang, N., 1997. Ozone exposure and population density in Harris County, Texas. J. Am. Stat. Assoc. 92,392–404.

Cooper, O.R., Gao, R.-S., Tarasick, D., Leblanc, T., Sweeney, C., 2012. Long-term ozone trends at rural ozone monitoring sites across the United States, 1990–2010. J. Geophys. Res. 117, D22307.

Dawson, J.P., Bloomer, B.J., Winner, D.A., Weaver, C.P., 2014. Understanding the meteorological drivers of U.S. particulate matter concentrations in a changing climate. Bull. Am. Meteorol. Soc. 95, 521-532.

Dittenhoefer, A.C., Pena, R.G. de, 1978. A study of production and growth of sulphate particles in plumes from a coal-fired power plant. Atmos. Environ. 12, 297–306.

Eder, B.K., Davis, J.M., Bloomfield, P., 1994. An automated classification scheme designed to better elucidate the dependence of ozone on meteorology. J. Appl. Meteorol. 33, 1182–1199.

EPA, 2004. Air quality criteria for particulate matter. Washington, DC. EPA 600/P-99/002aF-bF. https://cfpub.epa.gov/ncea/risk/recordisplay.cfm?deid=87903

EPA, 2005. Particulate matter health risk Assessment for selected urban Areas. Research Triangle Park, NC. https://www3.epa.gov/ttn/naaqs/standards/pm/data/pm_risk_tsd_finalreport_2005_mainbody.pdf

EPA, 2007. Review of the national ambient air quality standards for ozone: policy assessment of scientific and technical information. Research Triangle Park, NC. https://www3.epa.gov/ttn/naaqs/standards/ozone/data/2007_07_ozone_staff_paper.pdf

EPA, 2014. Regulatory impact analysis of the proposed revisions to the national ambient air quality standards for ground-level ozone. Research Triangle Park, NC. https://www3.epa.gov/ttn/ecas/regdata/RIAs/20141125ria.pdf

Feng, X., Wang, S., 2012. Influence of different weather events on concentrations of particulate matter with different sizes in Lanzhou, China. J. Environ. Sci. 24, 665–674.

Frost, G., et al., 2006. Effects of changing power plant NOx emissions on ozone in the eastern United States: Proof of concept. J. Geophys. Res. 111, D12306.

Galbally, I.E., Roy, C.R., 1980. Destruction of ozone at the earth's surface. Q. J. R. Meteorol. Soc. 106, 599–620.

Garland, J.A., Derwent, R.G., 1979. Destruction at the ground and the diurnal cycle of concentration of ozone and other gases. Q. J. R. Meteorol. Soc. 105, 169–183.

Gilliland, A.B., Hogrefe, C., Pinder, R.W., Godowitch, J.M., Foley, K.L., Rao, S.T., 2008. Dynamic evaluation of regional air quality models: Assessing changes in O3 stemming from changes in emissions and meteorology. Atmos. Environ. 42, 5110–5123.

Goliff, W.S., Stockwell, W.R., Lawson, C.V., 2013. The regional atmospheric chemistry mechanism, Version 2. Atmos. Environ. 68, 174–185.

Green, M.C., Chow, J.C., Watson, J.G., Dick, K., Inouye. D., 2015. Effect of snow cover and atmospheric stability on winter PM2.5 concentrations in western US valleys. J. Appl. Meteorol. Climatol. 54, 1191–1201.

Horton, D.E., Harshvardhan, Diffenbaugh, N.S., 2012. Response of air stagnation frequency to anthropogenically enhanced radiative forcing. Environ. Res. Lett. 7, 044034.

IPCC, 2007. Climate change 2007: Impacts, adaptation and vulnerability. Contribution of Working Group II to the Fourth Assessment Report of the Intergovernmental Panel on Climate Change. Cambridge University Press, Cambridge, UK, 976pp.

Jacob, D.J., Winner, D.A., 2009. Effect of climate change on air quality. Atmos. Environ. 43, 51–63.

Kim, S.-W., Heckel, A., McKeen, S.A., Frost, G.J., Hsie, E.-Y., Trainer, M.K., Richter, A., Burrows, J.P., Peckham, S. E., Grell, G.A., 2006. Satellite-observed U.S. power plant NOx emission reductions and their impact on air quality. Geophys. Res. Lett. 33, L22812.

Klingberg, J., Karlsson, P.E., Pihl Karlsson, G., Hu, Y., Chen, D., Pleijel, H., 2012. Variation in ozone exposure in the landscape of southern Sweden with consideration of topography and coastal climate. Atmos. Environ. 47, 252–260.

Koch, D., Park, J., Genio, A. Del, 2003. Clouds and sulfate are anticorrelated: A new diagnostic for global sulfur models. J. Geophys. Res. 108, No. D24, 4781.

Liebesch, E.J., Pena, R.G. de, 1982. Sulphate aerosol production in coal-fired power plant plumes. Atmos. Environ. 16, 1323–31.

Liu, W., Wang, Y., Russell, A., Edgerton, E., 2005. Atmospheric aerosols over two urban-rural pairs in southeastern United States: Chemical composition and sources. Atmos. Environ. 39, 4453–4470.

Melillo, J.M., Richmond, T.C., Yohe, G.W., Eds., 2014. Climate Change Impacts in the United States: The Third National Climate Assessment.

Niu, X.F., 1996. Nonlinear additive models for environmental time series with applications to ground-level ozone data analysis. J. Am. Stat. Assoc. 91, 1310–1321.

Oltmans, S. J., Levy II, H., 1992. Seasonal cycle of surface ozone over the western North Atlantic. Nature, 358, 392–394.

Pope, C.A., Dockery, D.W., 2006. Health effects of fine particulate air pollution: lines that connect. J. Air Waste Manag. Assco. 56, 709–742.

Prenni, A.J., Day, D.E., Evanoski-Cole, A.R., Sive, B.C., Hecobian, A., Zhou, Y., Gebhart, K.A., Hand, J.L., Sullivan, A.P., Li, Y., Schurman, M.I., Desyaterik, Y., Malm, W.C., Collet Jr., J.L., Schichtel, B.A., 2016. Oil and gas impacts on air quality in federal lands in the Bakken region: an overview of the Bakken Air Quality Study and first results. Atmos. Chem. Phys. 16, 1401–1416.

Rao, S.T., Zurbenko, I.G., Neagu, R., Porter, P.S., Ku, J.Y., Henry, R.F., 1997. Space and time scales in ambient ozone data. Bull. Am. Meteorol. Soc. 78, 2153–2166.

Robinson, P.J., 2001. On the definition of a heat wave. J. Appl. Meteorol. 40, 762-775.

Schnell, R.C., Oltmans, S.J., Neely, R.R., Endres, M.S., Molenar, I.V., White, A.B., 2009. Rapid photochemical production of ozone at high concentrations in a rural site during winter. Nat. Geosci. 2, 120–123.

Sheehan, P.E., Bowman, F.M., 2001. Estimated effects of temperature on secondary organic aerosol concentrations. Environ. Sci. Tech. 35, 2129–2135.

Stelson, A.W., Seinfeld, J.H., 1982. Relative humidity and temperature dependence of the ammonium nitrate dissociation constant. Atmos. Environ. 16, 983–992.

Tagaris, E., Liao, K.J., DeLucia, A.J., Deck, L., Russell, A.G., 2009. Potential impact of climate change on air pollution-related human health. Environ. Sci. Tech. 43, 4979–4988.

Tai, A., Mickley, L.J., Jacob, D.J., 2010. Correlations between fine particulate matter (PM2.5) and meteorological variables in the United States: Implications for the sensitivity of PM2.5 to climate change. Atmos. Environ. 44, 3976–3984.

Tang, L., Chen, D., Karlsson, P.E., Gu, Y., Ou, T., 2009. Synoptic circulation and its influence on spring and summer surface ozone concentrations in southern Sweden. Boreal Env. Res. 14, 889–902.

Thompson, M. L., 2001. A review of statistical methods for the meteorological adjustment of tropospheric ozone. Atmos. Environ. 35, 617–630.

Wang, J.X.L., Angell, J.K., 1999. Air stagnation climatology for the United States (1948-1998). NOAA/Air Resources Laboratory ATLAS, No.1.

WHO, 2014. Ambient (outdoor) air quality and health, Fact sheet N°313. http://www.who.int/mediacentre/factsheets/fs313/en/

Zeng, T., Wang, Y., Yoshida, Y., Tian, D., Russell, A.G., Barnard, W.R., 2008. Impacts of prescribed fires on air quality over the southeastern United States in spring based on modeling and ground/satellite measurements. Environ. Sci. Tech. 42, 8401–8406.

Zeng, T., Wang, Y., 2011. Biomass burning induced nationwide summer peaks of OC/EC ratios in the continental United States. Atmos. Environ. 45, 578–586.

Zhang, J., Rao, S.T., 1999. The role of vertical mixing in the temporal evolution of ground-level ozone concentrations. J. Appl. Meteorol. 38, 1674–1691.

Table 1 Selected Air Quality Indices and Meteorological Parameters

Table 2a Correlation Coefficients of Extreme Weather Indices with Extreme Ozone Days for Four Types of Stations

Table 2b Correlation Coefficients of Extreme Weather Indices with Extreme PM2.5 Days for Four Types of Stations

Fig. 1. Temporal evolutions of (a) extreme ozone days, (b) extreme Tmax days, (c) extreme RHmin days, (d) extreme Vmin days, (e) heat wave days, (f) dry event days, (g) low wind event days, (h) overlapped extreme ozone and Tmax days, (i) overlapped extreme ozone and RHmin days, (j) overlapped extreme ozone and Vmin days, (k) overlapped extreme ozone and heat wave days, (l) overlapped extreme ozone and dry event days, and (m) overlapped extreme ozone and low wind event days, using data from 1297 stations that have coverage more than 20% of the entire 30-year period.

Fig. 2. Spatial distributions of correlation coefficients for (a) annual extreme ozone and Tmax days, (b) annual extreme ozone and RHmin days, and (c) annual extreme ozone and Vmin days.

Fig. 3. Frequency of occurrences of (a) extreme ozone days, and (b) extreme Tmax/Vmin/RHmin days, for the entire 30-year period, three decades, and four seasons. The numbers of overlapping ozone extreme days with the highest 5% (95% to 100%), medium 5% (47.5% to 52.5%), and lowest 5% (0 to 5%) of extreme Tmax days, RHmin days, Vmin days for various time periods and four seasons are shown in (c), (d), and (e), respectively. The percentage ratios of overlapped extreme Tmax days, RHmin days, and Vmin days to extreme ozone days to are shown in (f), (g), and (h), respectively.

Fig. 4. Spatial distributions of the percentage ratios of ozone extreme days overlapping with extreme Tmax days (left column), extreme RHmin days (middle column), and extreme Vmin

days (right column) for the entire 30 years (first row), winter (second row), spring (third row), summer (fourth row), and fall (fifth row).Fig. 5. Variations of ozone extreme days at EPA AQS stations averaged over the period of (a) 1980 to 2009, (b) 1980 to 1989, (c) 1990 to 1999, and (d) 2000 to 2009. The size of circle at each station represents the average number of ozone extreme days changing per year. The circle is filled with color red for an increasing trend and color blue for a decreasing trend. Different shades of color indicate the confidence level ranging from 80% to 100%. For example, a large deep red circle means the station experienced an increasing trend with average ozone event increasing at a 4.5 event per year rate and at a 99% confidence level. Color shading in (a) indicates the four regions: California (CA) in green, Northwest U.S. (NW) in yellow, Northeast U.S. (NE) in gray, and Southeast U.S. (SE) in light blue. Fig. 6. Joint PDF of extreme ozone days as a function of Tmax and RHmin (first column), Tmax and Vmin (second column), and RHmin and Vmin (third column) for the entire 30-year period (first row), winter (second row), spring (third row), summer (fourth row), and fall (fifth row).Fig. 7. Joint PDF of extreme ozone events to Tmax and RHmin for California (first column), Northwest U.S. (second column), Southeast U.S. (third column), and Northeast U.S. (last column) for the entire 30 years (first row), winter (second row), spring (third row), summer (fourth row), and fall (last row). The four regions were shown in Fig. 5a. Fig. 8. Temporal evolutions of (a) extreme PM2.5 days, (b) extreme Tmax days, (c) extreme RHmin days, (d) extreme Vmin days, (e) heat wave days, (f) dry event days, (g) low wind event days, (h) overlapped extreme PM2.5 and Tmax days, (i) overlapped extreme PM2.5 and RHmin days, (j) overlapped extreme PM2.5 and Vmin days, (k) overlapped extreme PM2.5 and heat wave days, (l) overlapped extreme PM2.5 and dry event days, and (m) overlapped extreme PM2.5 and low wind event days, using data from 788 stations that have data coverage more than 20% of the entire 10-year period. Fig. 9. Spatial distributions

of the correlation coefficients between (a) extreme PM2.5 and Tmax days, (b) extreme PM2.5 and RHmin days, and (c) extreme PM2.5 and Vmin days.Fig. 10. Frequency of occurrences for (a) extreme PM2.5 days, (b) extreme Tmax/Vmin/RHmin days, for the entire 10-year period and four seasons. The numbers of overlapping PM2.5 extreme days with the highest 5% (95% to 100%), medium 5% (47.5% to 52.5%), and lowest 5% (0 to 5%) of extreme Tmax days, RHmin days, and Vmin days for the entire 10-year period and four seasons are shown in (c), (d), and (e), respectively. The percentage ratios of overlapped extreme Tmax days, RHmin days, and Vmin days to extreme PM2.5 days are shown in (f), (g), and (h), respectively.Fig. 11. Spatial distributions of the percentage ratios of PM2.5 extreme days overlapping with Tmax (left column), RHmin (middle column), and Vmin (right column) at the top 5% (top row), medium 5% (middle row), and lower 5% (bottom row) range. Fig. 12. Variations of the PM2.5 extreme days at EPA AQS stations averaged over the 10-year period between 2000 and 2009. Similar to Fig. 6: The size of circle at each station represents the average number of events changing per year. Red color indicates an increasing trend and blue color indicates a decreasing trend. Different shades of color indicate the confidence level ranging from 80% to 100%. Fig. 13. Joint PDF of extreme PM2.5 days as a function of Tmax and RHmin (first column), Tmax and Vmin (second column), and RHmin and Vmin (third column) for the entire 10-year period (first row), winter (second row), spring (third row), summer (fourth row), and fall (fifth row).

Table 1 Selected Air Quality Indices and Meteorological Parameters

	Data Source	**Time Period**	**Number of AQS Stations or Model Grid Points**	**Extreme event threshold**
Ozone	EPA AQS 8-hr maximum ozone concentration (ppbv)	1980-2009	30 year: 1297 80s: 850 90s: 1104 00s: 1316 Winter (DJF*): 839 Spring (MAM): 1326 Summer(JJA): 1488 Fall (SON): 1303	95th percentile
PM2.5	EPA AQS PM2.5 24-hr geometric mean (ugm^{-3})	2000-2009	10 year: 788 Winter(DJF): 783 Spring(MAM): 784 Summer(JJA): 771 Fall(SON): 785	95th percentile
Tmax	NCEP CFSR daily maximum 2 meter temperature (K)	1980-2009	Closest grid point to a specific AQS station	95th percentile
RHmin	NCEP CFSR daily minimum 2 meter relative humidity	1980-2009	Closest grid point to a specific AQS station	5th percentile
Vmin	NCEP CFSR daily minimum 2 meter wind speed	1980-2009	Closest grid point to a specific AQS station	5th percentile

* Winter: December-January-Feburary (DJF); spring: March-April-May (MAM); summer: June-July-August (JJA); and fall: September-October-November (SON).

Table 2a Correlation Coefficients of Extreme Weather Indices with Extreme Ozone Days for Four Types of Stations

	Rural	**Suburban**	**Urban**	**Unknown**	**All**
Extreme Tmax days	0.448	0.524	0.586	0.101	0.532
Extreme RHmin days	0.534	0.453	0.554	0.233	0.540
Extreme Vmin days	–0.495	–0.316	0.201	–0.183	–0.282

Table 2b Correlation Coefficients of Extreme Weather Indices with Extreme PM2.5 Days for Four Types of Stations

	Rural	**Suburban**	**Urban**	**Unknown**	**All**
Extreme Tmax days	0.602	0.510	0.582	0.502	0.559
Extreme RHmin days	0.468	0.753	0.731	0.325	0.722
Extreme Vmin days	–0.693	–0.677	–0.138	–0.586	–0.504

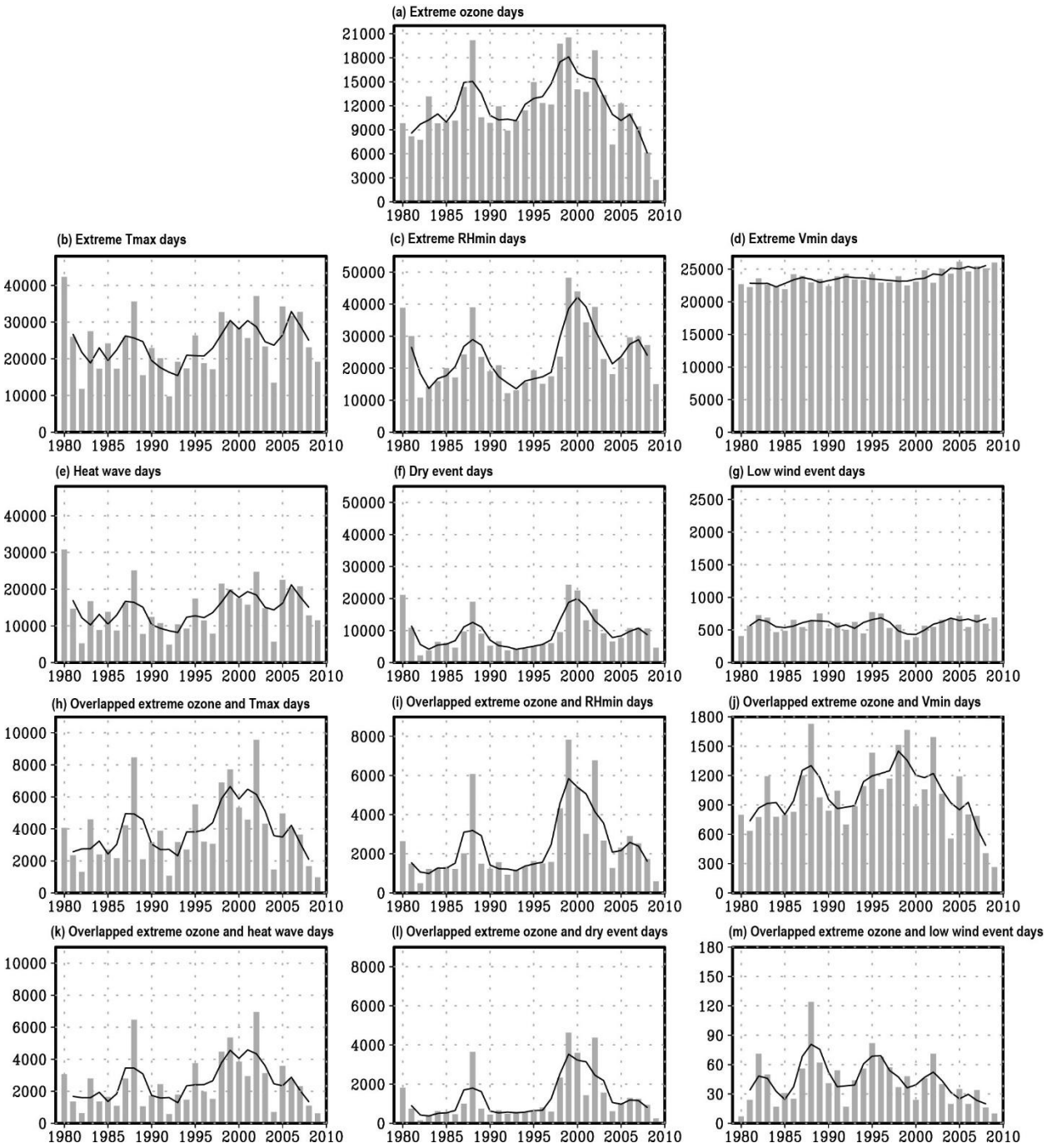

Fig. 1. Temporal evolutions of (a) extreme ozone days, (b) extreme Tmax days, (c) extreme RHmin days, (d) extreme Vmin days, (e) heat wave days, (f) dry event days, (g) low wind event days, (h) overlapped extreme ozone and Tmax days, (i) overlapped extreme ozone and RHmin days, (j) overlapped extreme ozone and Vmin days, (k) overlapped extreme ozone and heat wave days, (l) overlapped extreme ozone and dry event days, and (m) overlapped extreme ozone and low wind event days, using data from 1297 stations that have coverage more than 20% of the entire 30-year period.

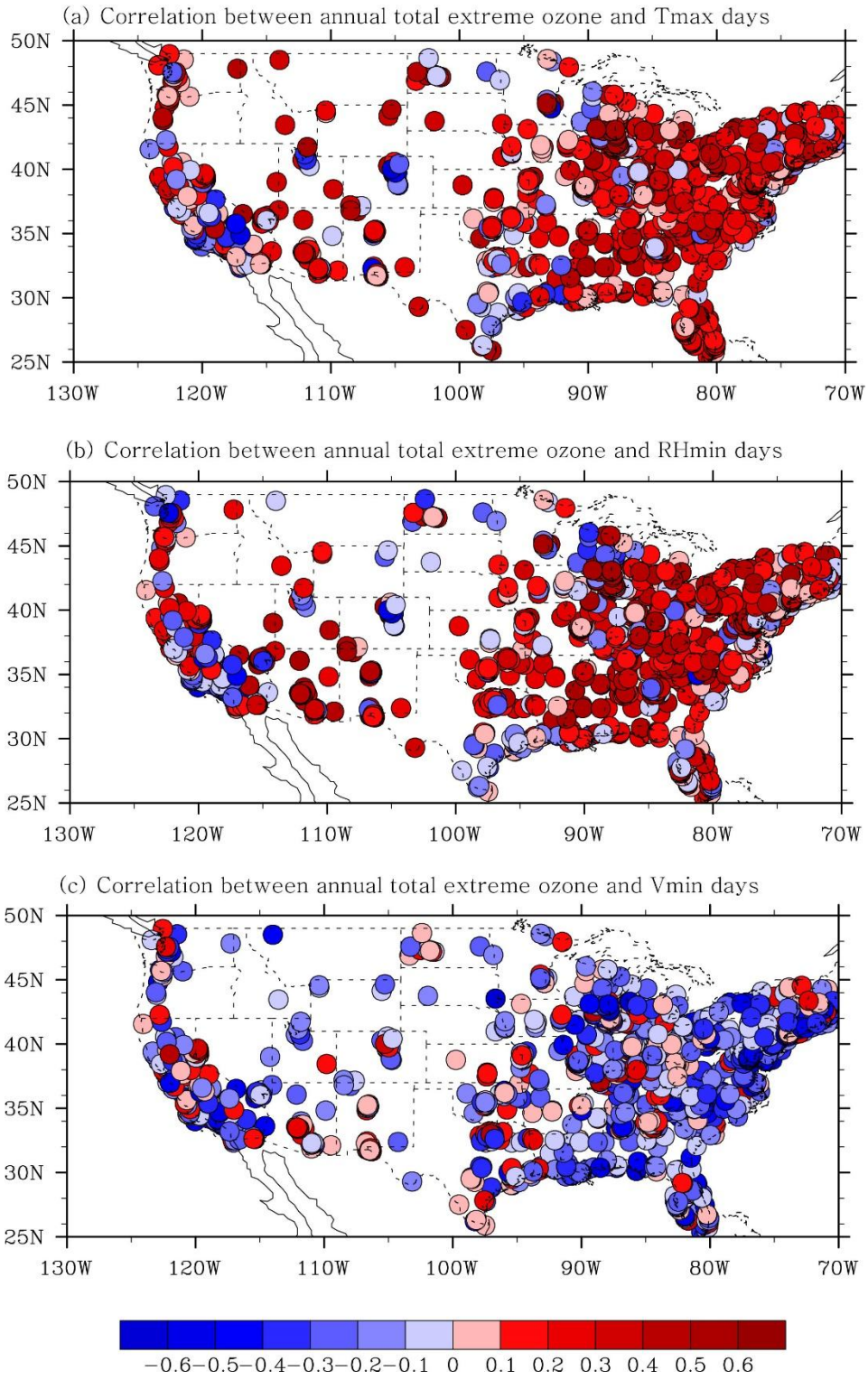

Fig. 2. Spatial distributions of correlation coefficients for (a) annual extreme ozone and Tmax days, (b) annual extreme ozone and RHmin days, and (c) annual extreme ozone and Vmin days.

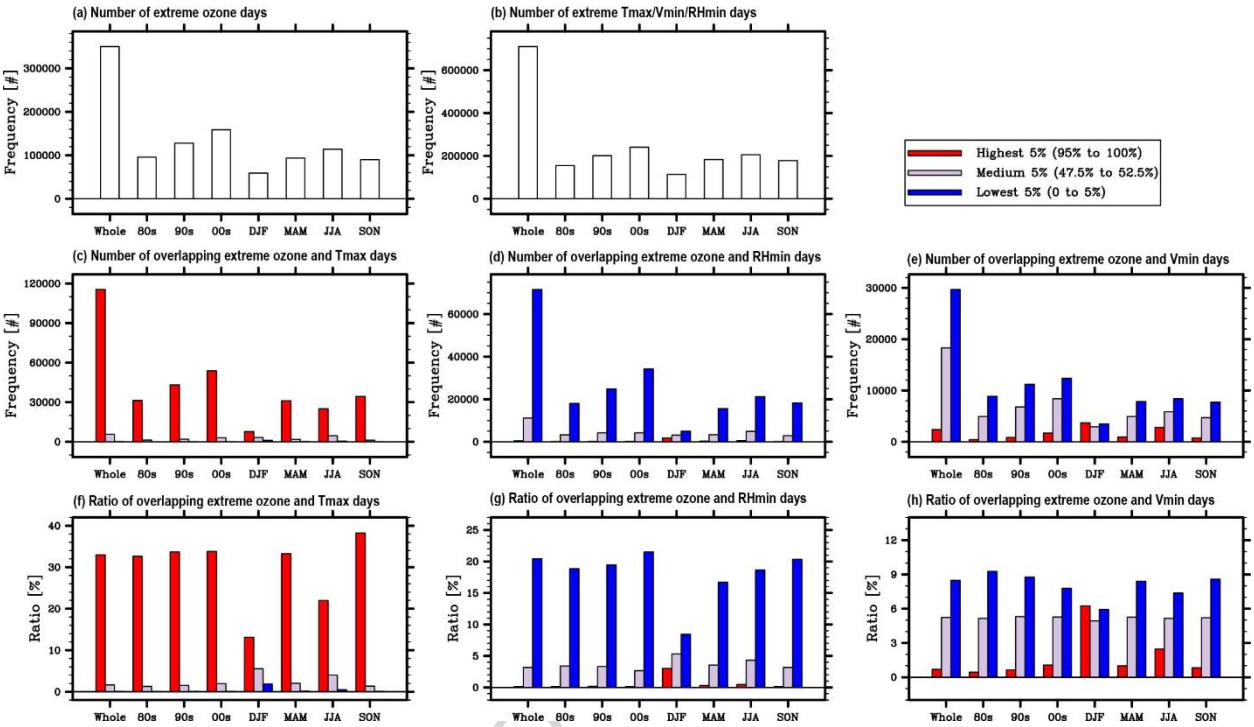

Fig. 3. Frequency of occurrences of (a) extreme ozone days, and (b) extreme Tmax/Vmin/RHmin days, for the entire 30-year period, three decades, and four seasons. The numbers of overlapping ozone extreme days with the highest 5% (95% to 100%), medium 5% (47.5% to 52.5%), and lowest 5% (0 to 5%) of extreme Tmax days, RHmin days, Vmin days for various time periods and four seasons are shown in (c), (d), and (e), respectively. The percentage ratios of overlapped extreme Tmax days, RHmin days, and Vmin days to extreme ozone days to are shown in (f), (g), and (h), respectively.

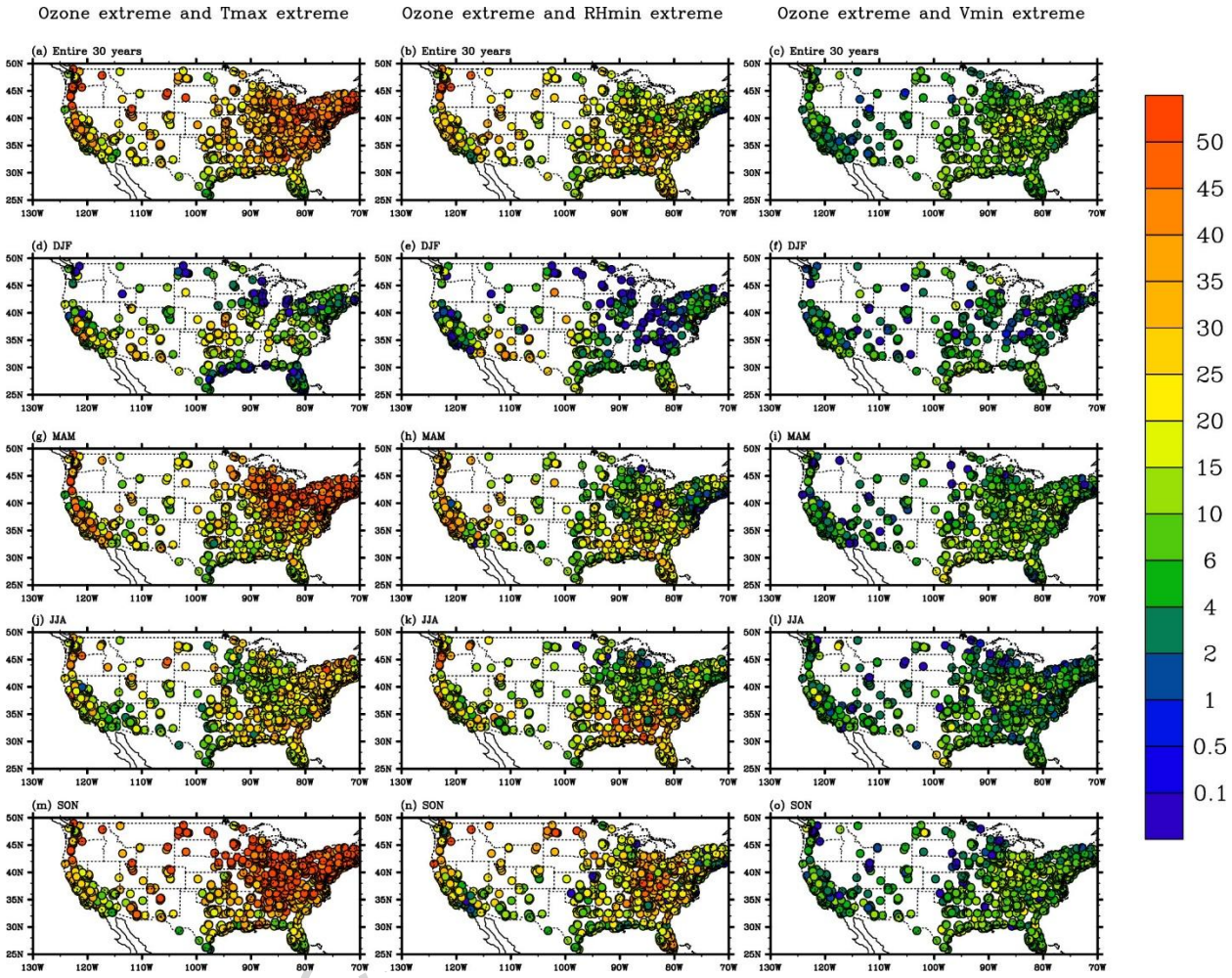

Fig. 4. Spatial distributions of the percentage ratios of ozone extreme days overlapping with extreme Tmax days (left column), extreme RHmin days (middle column), and extreme Vmin days (right column) for the entire 30 years (first row), winter (second row), spring (third row), summer (fourth row), and fall (fifth row).

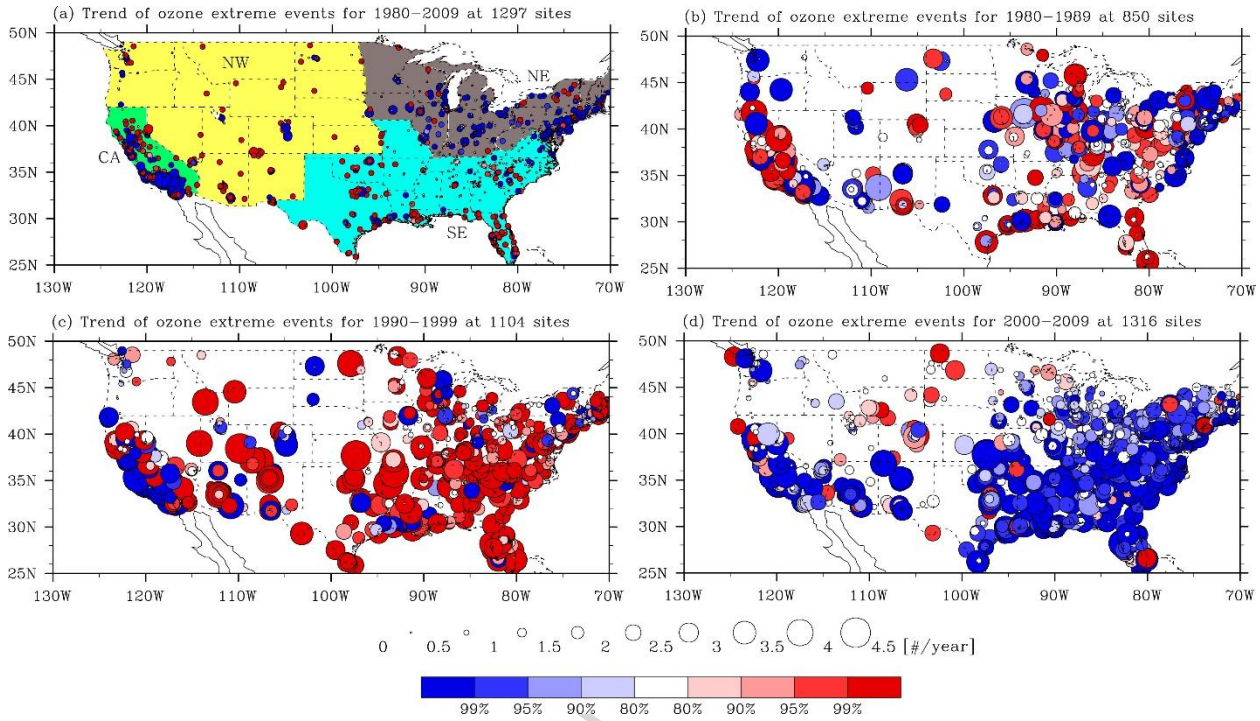

Fig. 5. Variations of ozone extreme days at EPA AQS stations averaged over the period of (a) 1980 to 2009, (b) 1980 to 1989, (c) 1990 to 1999, and (d) 2000 to 2009. The size of circle at each station represents the average number of ozone extreme days changing per year. The circle is filled with color red for an increasing trend and color blue for a decreasing trend. Different shades of color indicate the confidence level ranging from 80% to 100%. For example, a large deep red circle means the station experienced an increasing trend with average ozone event increasing at a 4.5 event per year rate and at a 99% confidence level. Color shading in (a) indicates the four regions: California (CA) in green, Northwest U.S. (NW) in yellow, Northeast U.S. (NE) in gray, and Southeast U.S. (SE) in light blue.

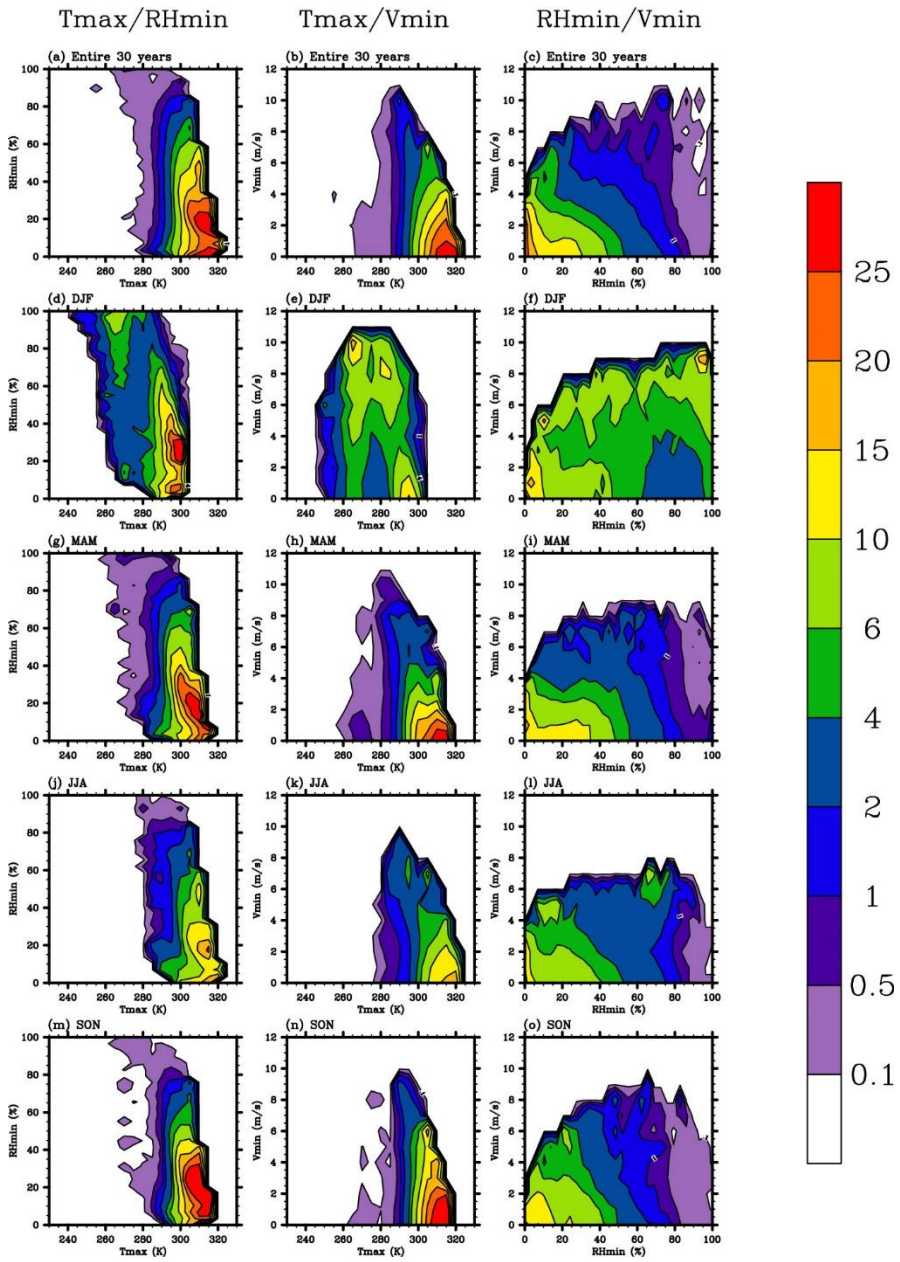

Fig. 6. Joint PDF of extreme ozone days as a function of Tmax and RHmin (first column), Tmax and Vmin (second column), and RHmin and Vmin (third column) for the entire 30-year period (first row), winter (second row), spring (third row), summer (fourth row), and fall (fifth row).

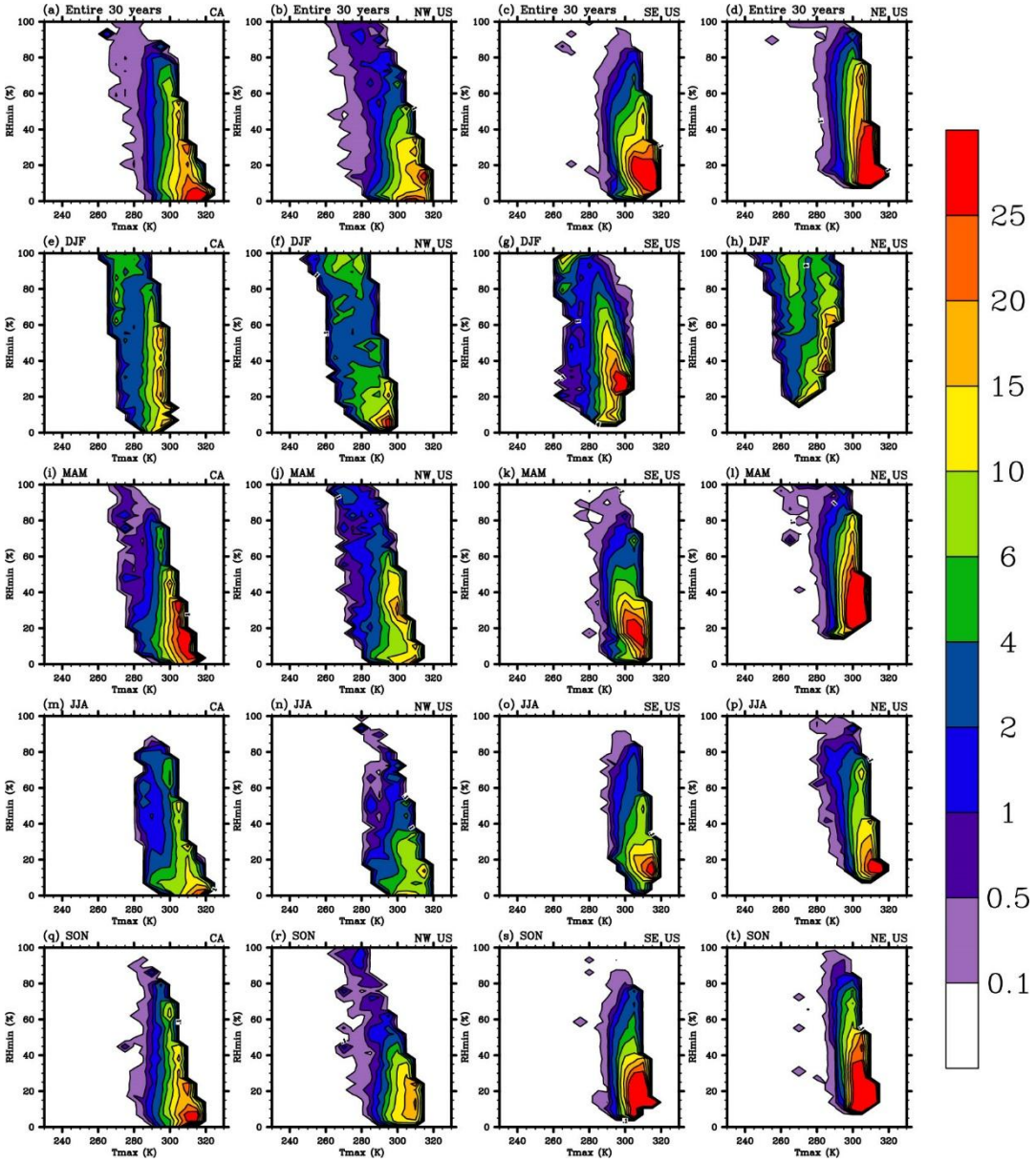

Fig. 7. Joint PDF of extreme ozone events to Tmax and RHmin for California (first column), Northwest U.S. (second column), Southeast U.S. (third column), and Northeast U.S. (last column) for the entire 30 years (first row), winter (second row), spring (third row), summer (fourth row), and fall (last row). The four regions were shown in Fig. 5a.

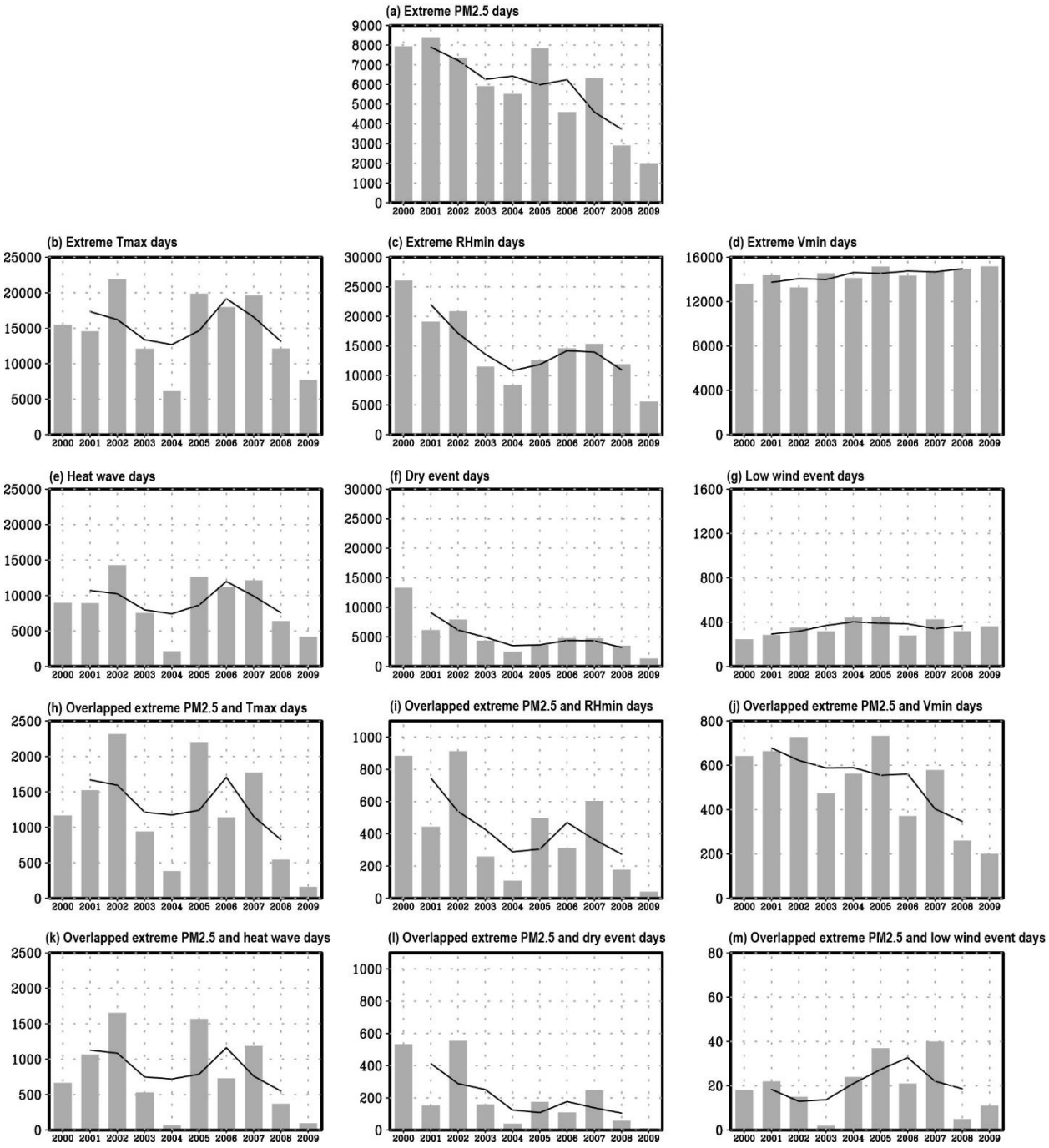

Fig. 8. Temporal evolutions of (a) extreme PM2.5 days, (b) extreme Tmax days, (c) extreme RHmin days, (d) extreme Vmin days, (e) heat wave days, (f) dry event days, (g) low wind event days, (h) overlapped extreme PM2.5 and Tmax days, (i) overlapped extreme PM2.5 and RHmin days, (j) overlapped extreme PM2.5 and Vmin days, (k) overlapped extreme PM2.5 and heat wave days, (l) overlapped extreme PM2.5 and dry event days, and (m) overlapped extreme PM2.5 and low wind event days, using data from 788 stations that have data coverage more than 20% of the entire 10-year period.

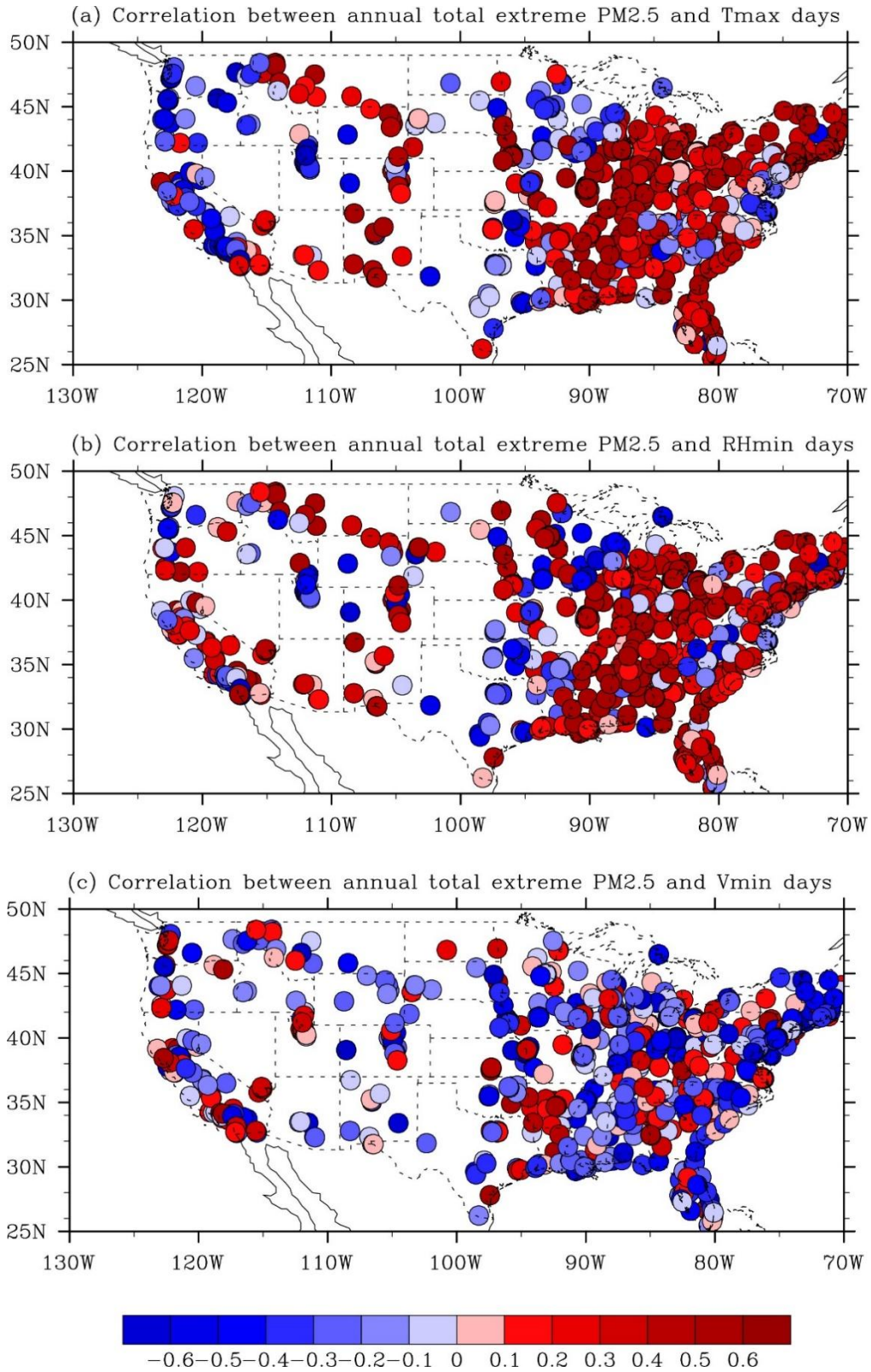

Fig. 9. Spatial distributions of the correlation coefficients between (a) extreme PM2.5 and Tmax days, (b) extreme PM2.5 and RHmin days, and (c) extreme PM2.5 and Vmin days.

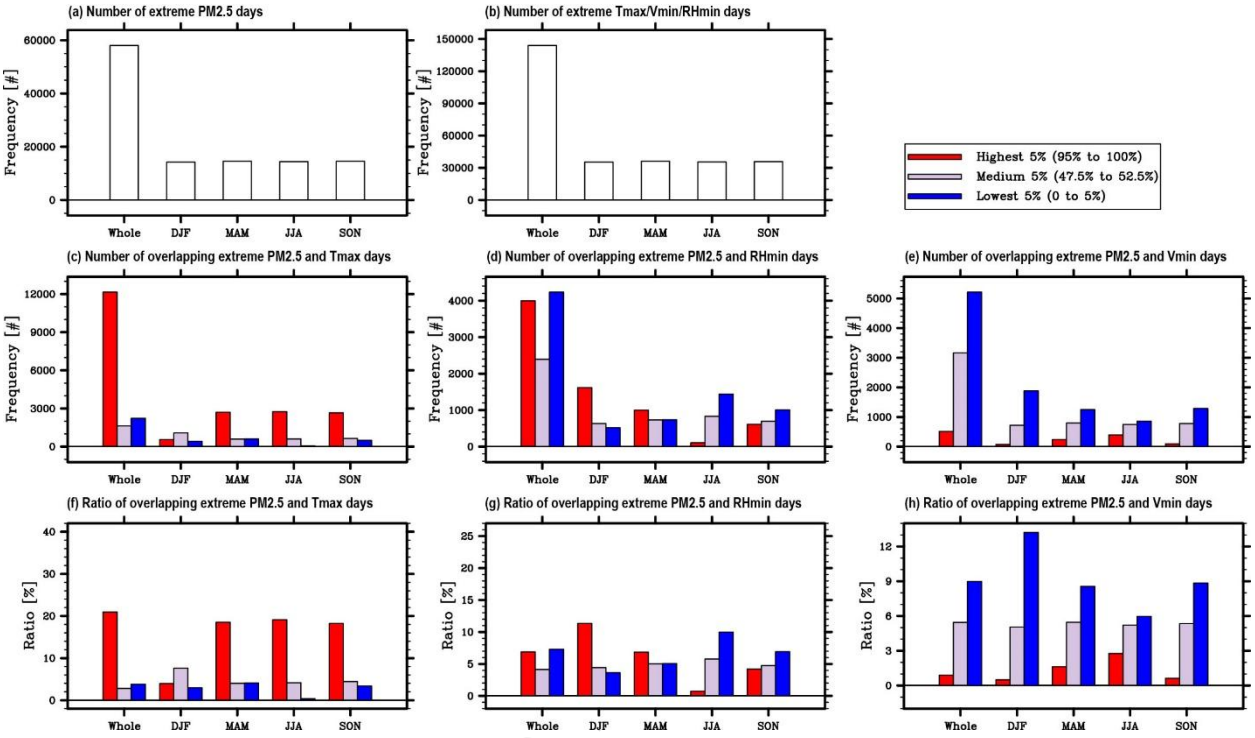

Fig. 10. Frequency of occurrences for (a) extreme PM2.5 days, (b) extreme Tmax/Vmin/RHmin days, for the entire 10-year period and four seasons. The numbers of overlapping PM2.5 extreme days with the highest 5% (95% to 100%), medium 5% (47.5% to 52.5%), and lowest 5% (0 to 5%) of extreme Tmax days, RHmin days, and Vmin days for the entire 10-year period and four seasons are shown in (c), (d), and (e), respectively. The percentage ratios of overlapped extreme Tmax days, RHmin days, and Vmin days to extreme PM2.5 days are shown in (f), (g), and (h), respectively.

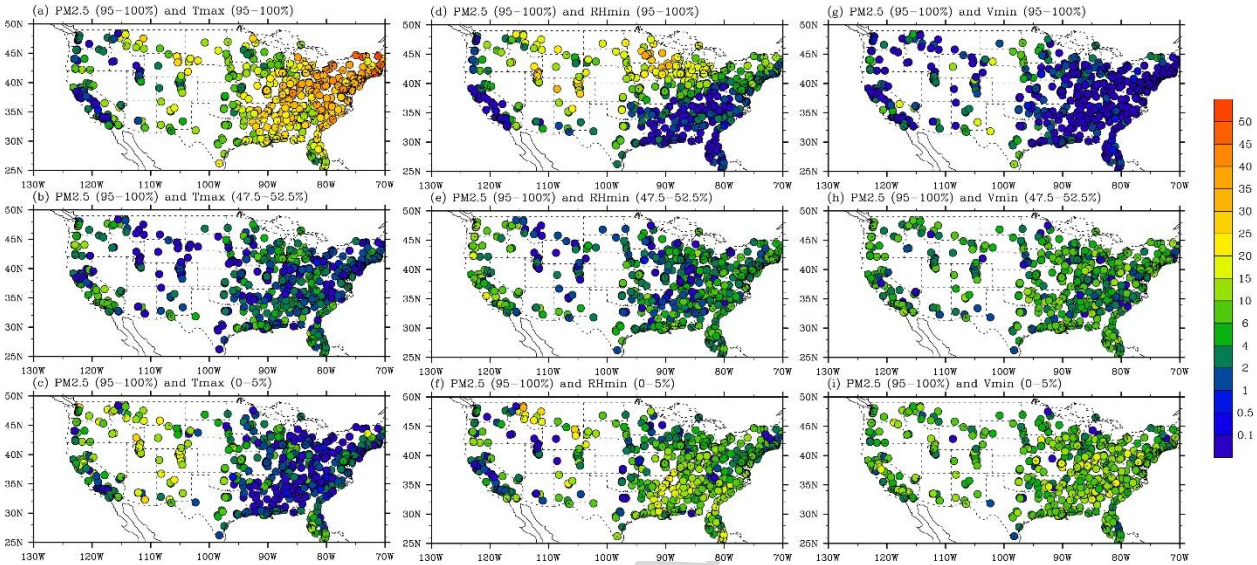

Fig. 11. Spatial distributions of the percentage ratios of PM2.5 extreme days overlapping with Tmax (left column), RHmin (middle column), and Vmin (right column) at the top 5% (top row), medium 5% (middle row), and lower 5% (bottom row) range.

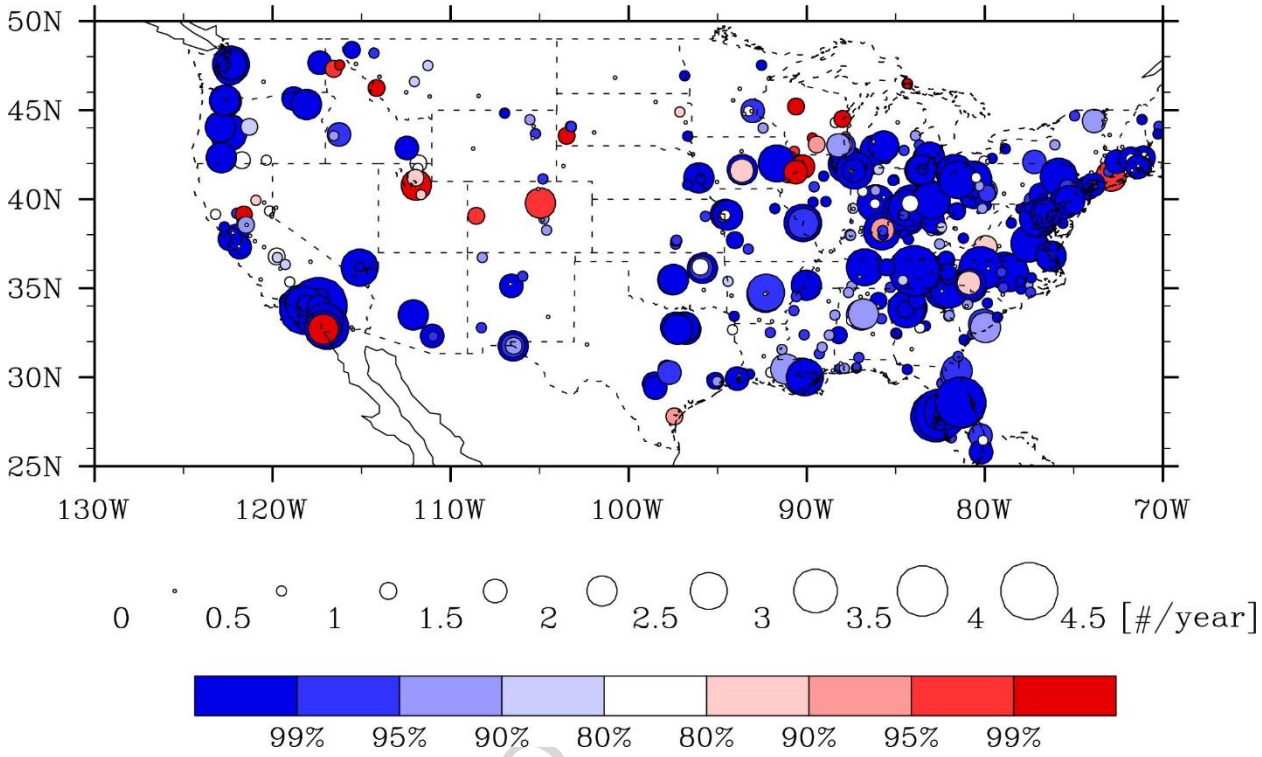

Fig. 12. Variations of the PM2.5 extreme days at EPA AQS stations averaged over the 10-year period between 2000 and 2009. Similar to Fig. 5: The size of circle at each station represents the average number of events changing per year. Red color indicates an increasing trend and blue color indicates a decreasing trend. Different shades of color indicate the confidence level ranging from 80% to 100%.

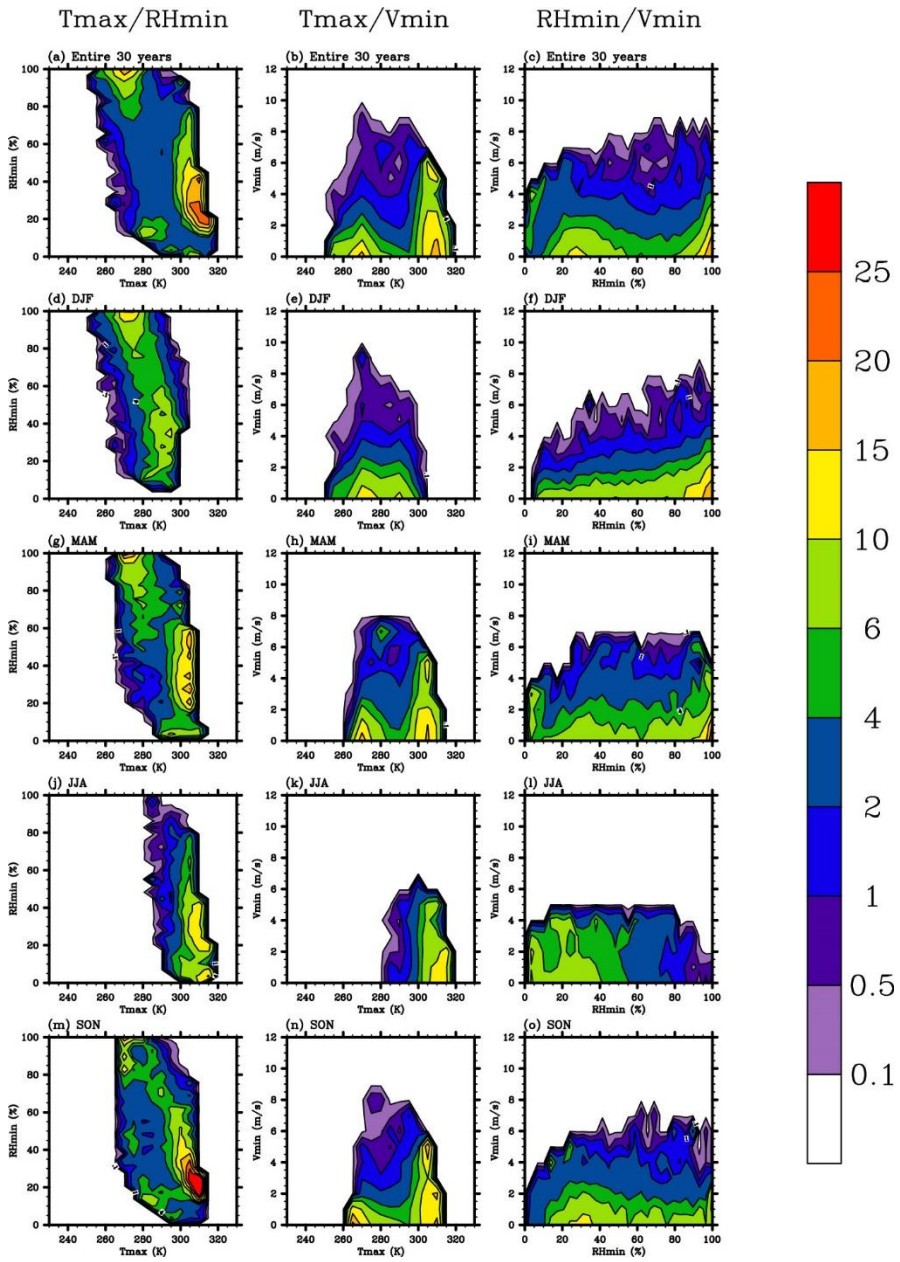

Fig. 13. Joint PDF of extreme PM2.5 days as a function of Tmax and RHmin (first column), Tmax and Vmin (second column), and RHmin and Vmin (third column) for the entire 10-year period (first row), winter (second row), spring (third row), summer (fourth row), and fall (fifth row).

Highlights

Title: Quantifying the Relationship between Extreme Air Pollution Events and Extreme Weather Events

Authors: Henian Zhang, Yuhang Wang, Tae-Won Park, and Yi Deng

Highlights:

- Developed a new statistical method to quantify the ozone/PM2.5 and weather extremes.
- Ozone/PM2.5 extremes were most sensitive to temperature extremes on an annual basis.
- Annual PM2.5 extremes highly correlated with low RH days in urban/suburban areas.
- Fewer ozone/PM2.5 extremes in suburban and rural areas when wind speeds were low.